



## Synthesis and Characterization of Se Doped $\text{Bi}_2\text{Te}_3$ Nanocrystalline Materials

*Se Katkılı  $\text{Bi}_2\text{Te}_3$  Nanokristal Materyallerin Sentezi ve Karakterizasyonu*

Hayati Mamur<sup>1,\*</sup> M.R.A. Bhuiyan<sup>2</sup>

<sup>1</sup>Manisa Celal Bayar University, Faculty of Engineering, Electrical and Electronic Engineering Department, Manisa, Turkey

<sup>2</sup>Islamic University, Faculty of Engineering and Technology, Electrical and Electronic Engineering Department, Kushtia, Bangladesh

### Abstract

In this study, the selenium (Se) doped bismuth telluride ( $\text{Bi}_2\text{Te}_3$ ) nanocrystalline material synthesis by using a simple chemical route was presented. The bismuth (III) nitrate pentahydrate  $\text{Bi}(\text{NO}_3)_3 \cdot 5\text{H}_2\text{O}$ , telluride dioxide  $\text{TeO}_2$  and Se powder were dissolved by nitric acid  $\text{HNO}_3$ . Herein, the two-step co-precipitation chemical route by using the sodium hydroxide  $\text{NaOH}$  and sodium borohydride  $\text{NaBH}_4$  was employed. Different types of characterization such as X-ray diffraction (XRD), scanning electron microscopy (SEM), energy dispersive X-ray (EDX), transmission electron microscopy (TEM), atomic force microscopy (AFM), ultraviolet absorbance (UV) and Fourier transform infrared spectrometry (FT-IR) were occupied to the  $\text{Bi}_{2-x} \text{Se}_{0.6}$  nanocrystalline powders and pellets which were developed. According to the measurement results,  $\text{Bi}_{2-x} \text{Se}_{0.6}$  thermoelectric material was obtained in nano dimensions.

**Keywords:** Chemical route, Nanocrystalline powders, Se doped  $\text{Bi}_2\text{Te}_3$

### Öz

Bu çalışmada, basit bir kimyasal yol kullanılarak gerçekleştirilen selenyum (Se) katkılı bizmut tellürür ( $\text{Bi}_2\text{Te}_3$ ) nanokristalin malzeme sentezi sunulmuştur. Bizmut (III) nitrat pentahidrat  $\text{Bi}(\text{NO}_3)_3 \cdot 5\text{H}_2\text{O}$ , tellürür dioksit  $\text{TeO}_2$  ve Se tozu nitrik asit  $\text{HNO}_3$  ile çözülmüştür. Burada, sodyum hidrokсид  $\text{NaOH}$  ve sodyum borohidrid  $\text{NaBH}_4$  kullanılarak iki aşamalı birlikte çökeltme kimyasal yolu denenmiştir. Bunun sonucunda, geliştirilen  $\text{Bi}_{2-x} \text{Se}_{0.6}$  nanokristalin tozları ve peletlerinin ölçümleri için X-ışını kırınımı (XRD), taramalı elektron mikroskopisi (SEM), enerji dağılımlı X-ışını (EDX), transvers elektron mikroskopu (TEM), atomik kuvvet mikroskopu (AFM), ultraviyole absorbansı (UV) ve Fourier dönüşümü kızılötesi spektrometresi (FT-IR) cihazları kullanılmıştır. Elde edilen ölçüm sonuçlarına göre nano boyutlarda  $\text{Bi}_{2-x} \text{Se}_{0.6}$  termoelektrik maddesi elde edilmiştir.

**Anahtar Kelimeler:** Kimyasal yol, Nanokristalin tozlar, Se katkılı  $\text{Bi}_2\text{Te}_3$

### 1. Introduction

Recently, alternative technologies for improvement the thermal to electrical conversion efficiency of thermoelectric (TE) materials and devices have been studied. The  $\text{Bi}_2\text{Te}_3$  alloys are the new alternative TE materials as clean energy resources. The direct conversion from thermal to electrical energy can be easily realized in TE materials such as Se doped  $\text{Bi}_2\text{Te}_3$  (Kumar et al. 2017, Şişman and Başoğlu 2016, Zhang et al. 2011). Thanks to their particular nature, they can expand the possibilities for waste heat recovery applications. These materials have been worked on by many researchers to improve their thermal and electrical properties (Ivanova

et al. 2017, Klimovskikh et al. 2017, Meroz et al. 2016). Moreover, these studies show how a good TE material can be developed.

TE materials hold the key to the essential ahead in energy alteration and storage, both of which are crucial in order to meet the protest of universal heating and the finite nature of fossil fuels. The characterization of nanostructure materials represents an enormous challenge as the structured and crystalline dimension are beyond the structural and optical view (Ju and Kim 2016, Nomura et al. 2015, Park et al. 2016). Nanostructured materials are unnaturally formed materials. They have constitutive phase or grain structures modulated on a dimension less than 100 nm. They are manufactured by means of different ways such as chemical, mechanical and physical methods (Bisquert 2008, Huang and Choi 2007, Lu and Lu 2004.). Some nano scale materials can

\*Corresponding author: [hayati.mamur@cbu.edu.tr](mailto:hayati.mamur@cbu.edu.tr)

Hayati Mamur [orcid.org/0000-0001-7555-5826](https://orcid.org/0000-0001-7555-5826)  
M.R.A. Bhuiyan [orcid.org/0000-0001-7335-4158](https://orcid.org/0000-0001-7335-4158)

also be formed by means of more conventional methods. Nanostructure materials that involve multiple phases can range from the most conventional case. In which, a nano scale phase is inserted in a phase of traditional dimension to the case, in which all the constituent phases are of nano scale dimensions. All nanostructure materials share the properties: atomic domains spatially bordered to less than 100 nm. There are the significant atom fractions that are associated with interfacial environment and interactions between their consequences domains.

In recent years, nanostructured materials have begun to attract a great deal of attention. Because nanostructured materials have begun to be created by thoughtful scientists who will bring more advantages over materials made with other traditional products. Moreover, it is possible for the scientists these properties by controlling and varying the dimension of the constituent domains. This interest has been stimulated by not only the recent efforts and successes but also the rapid developments. Chemical solution co-precipitation method, one of the methods of producing nano materials, has been employed for producing of single phase Se doped Bi<sub>2</sub>Te<sub>3</sub> nanostructure which has low crystalline dimension. These methods have a sensitive control of the crystalline dimension, structure distribution and crystallinity. According to authors' previous reports (Barman et al. 2016, Bhuiyan et al. 2014, Bhuiyan and Mamur 2016, Mamur et al. In Press), this method has been suitable for the nanostructure material production when compared with electrochemical synthesis (Bhuiyan et al. 2012, Bhuiyan et al. 2017, Bhuiyan and Rahman 2014.). In this paper, the basic principles underlying the synthesis of nanostructure materials are shown. Also, this paper describes the Se doped Bi<sub>2</sub>Te<sub>3</sub> nanostructure development and characterization.

## 2. Material and Methods

### 2.1. Growth of Se Doped Bi<sub>2</sub>Te<sub>3</sub> Powder and Pellet

The reagents of bismuth (III) nitrate pentahydrate Bi(NO<sub>3</sub>)<sub>3</sub>.5H<sub>2</sub>O ( $\geq 98\%$ ), tellurium dioxide TeO<sub>2</sub> ( $\geq 97\%$ ) and Selenium powder Se ( $\geq 99.99\%$ ) were taken from Sigma-Aldrich. They were fulfilled as precursor materials for the co-precipitation of a simple chemical solution process. The solvents of HNO<sub>3</sub> ( $\sim 70\%$ , Sigma-Aldrich), NaOH (98–100 %, Sigma-Aldrich), NaBH<sub>4</sub> (98–100 %, mark) and Ethanol (Analytical grade, Mark) were also purchased. They were also employed without any further purification. In advance of the synthesis of Se doped Bi<sub>2</sub>Te<sub>3</sub>, nanopowders, Bi(NO<sub>3</sub>)<sub>3</sub>.5H<sub>2</sub>O, TeO<sub>2</sub> and Se were utilized as

the precursor in this process. The precursors were taken with stoichiometric ratio of Bi<sub>2</sub>Te<sub>2.4</sub>Se<sub>0.6</sub> for the co-precipitation. NaOH was applied for a regulated the p<sup>H</sup> value of the solution. NaBH<sub>4</sub> was employed as a reducing agent for removing the oxidization.

These chemicals were weighed according to their stoichiometry. Later, they were prepared separate metal ion solutions by using 2 mmol (0.97 gm) Bi(NO<sub>3</sub>)<sub>3</sub>.5H<sub>2</sub>O, 2.4 mmol (0.38304 gm) TeO<sub>2</sub> and 0.6 mmol (.047376 gm) Se powder. After that, these were dissolved in a concentrated (2 M = 31.86 ml) HNO<sub>3</sub>. A stock solution of (3 M = 30 gm) NaOH was added for regulating p<sup>H</sup> value. These three metallic solutions were reserved in one flux (solution 1) and other flux was fulfilled with NaOH solution (solution 2). Furthermore, these solutions were mixed together at room temperature with adjusting the hydro-dynamic atmosphere. Then, a complete co-precipitation was developed by a magnetic stirring for half an hour. The developed white precipitates are shown in Figure 1. The oxides were eliminated by using NaBH<sub>4</sub>. 150 ml white precipitate which was reserved in a borosilicate flux (solution 3) at 80°C by using the magnetic stirrer machine for several minutes. Other flux was carried out by means of 15 mmol (1.134 gm) NaBH<sub>4</sub> solution of 100ml distilled water at 80°C soluble by magnetic stirrer for 15 minutes (solution 4). Lastly, the solution 3 and 4 were mixed together at 80°C with adjusting the hydro-dynamic atmosphere. Schematic drawing of this solution route is shown in Figure 2.

The complete co-precipitation was developed by magnetic stirrer for eight hours to remove the oxidization. The developed black precipitates were collected by 6000 rpm speed centrifugation, washed several times with distilled water and pure ethanol and finally dried at 80°C for ~18 hours in an oven. Then the dried precursor which was collected was calcined in a vacuum furnace at 180°C for two hours. There after black colour Se doped Bi<sub>2</sub>Te<sub>3</sub> powder was developed that is sequentially shown in Figure 1.

A computer controlled 99% pure hydrogen (H<sub>2</sub>) gas at ~250°C was passed throughout the developed powder in order to overcome or minimize the oxidization. Finally, the nanocrystalline Bi<sub>2</sub>Te<sub>2.4</sub>Se<sub>0.6</sub> powders were synthesized successfully by using a chemical solution route.

In the end, the Bi<sub>2</sub>Te<sub>2.4</sub>Se<sub>0.6</sub> product powders were put in 1 cm diameter pellet base and pressed with 5 MPa pressure, which is shown in Figure 3. Then, they were collected. The pellet was heated in a vacuum furnace at 180°C for two

hours. Finally, the Se doped Bi<sub>2</sub>Te<sub>3</sub> nanostructure pellet, which is 1 cm diameter, .05 mm thickness, was developed for AFM measurement.

## 2.2. Experimental Details

The XRD patterns were recorded by using an X'Pert high

score PANalytical diffractometer with Cu-K $\alpha$  radiation, operated at 45 kV and 40 mA, with angular range  $20^\circ \leq 2\theta \leq 80^\circ$ . The morphology and elemental atomic composition of the sample were also accomplished with a scanning electron microscopy (SEM) and energy dispersive X-ray spectroscopy (EDX) of LEO 1430 VP system. For defining the variations

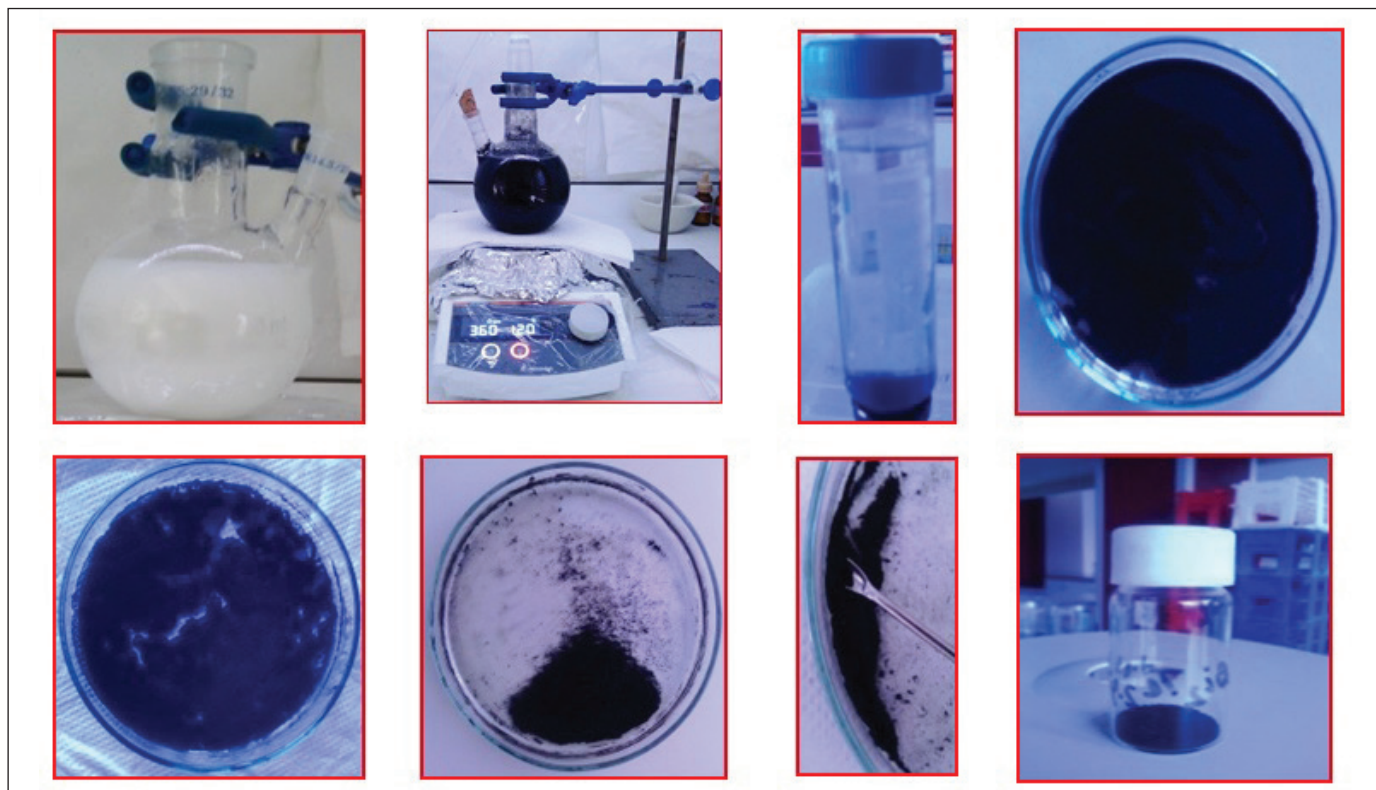


**Figure 1.** Synthesis of Se doped Bi<sub>2</sub>Te<sub>3</sub> nanopowders.

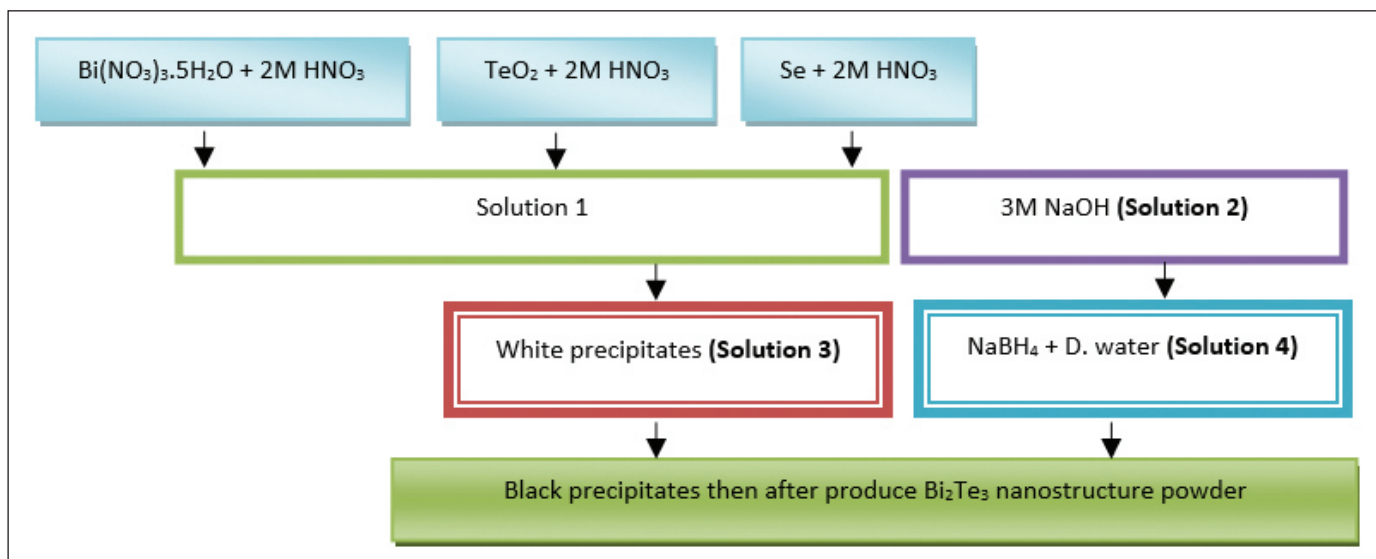


**Figure 2.** Schematic drawing of this solution route.

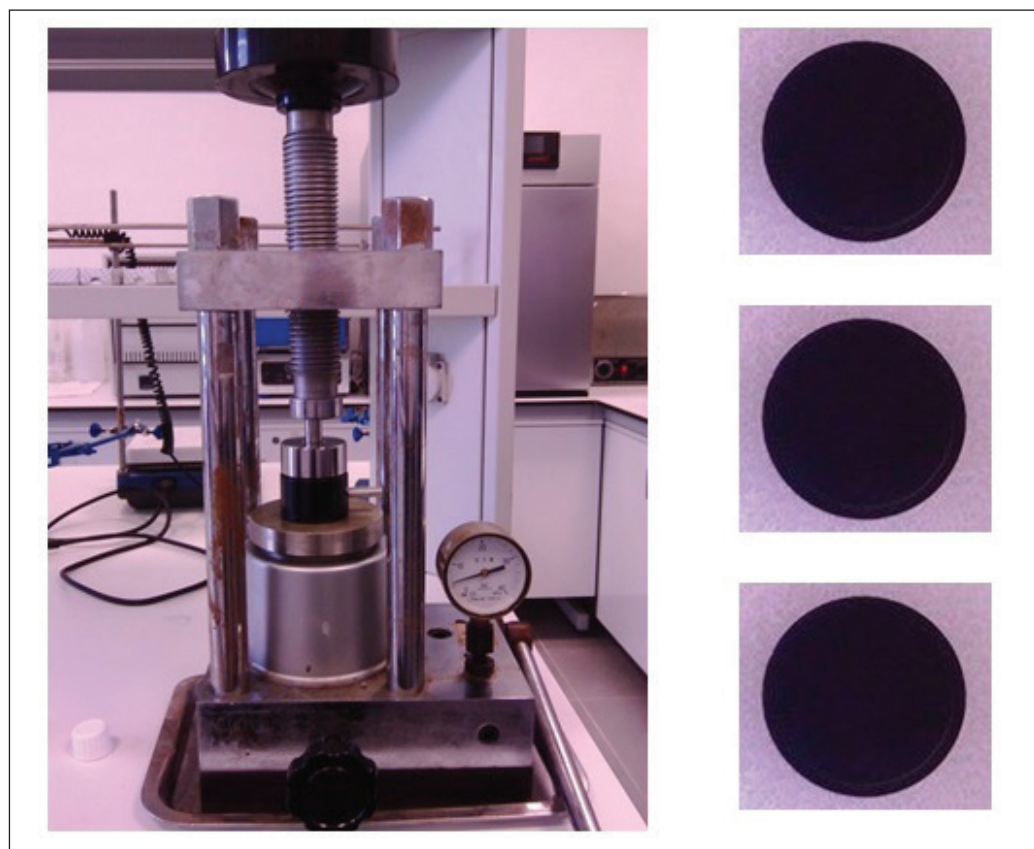


**Figure 3.** The Bi<sub>2</sub>Te<sub>2.4</sub>Se<sub>0.6</sub> nanostructure powders convert to pellet.

in synthesized Se doped morphology Bi<sub>2</sub>Te<sub>3</sub> nanostructure, transmission electron microscopy (TEM) measurement was utilized. It has field emission property. Moreover, it was operated at 200 kV. Its branding name was JEOL JEM 2100F HRTEM Microscope. The 3D topographic surfaces were recorded in 0.01 nm discrimination using 10 MP CCD cameras by an atomic force microscopy (AFM). The UV absorption was measured by using a UV-1800 recording spectrophotometer in the photon wavelength range from 200 to 800 nm. In addition, a BRUKER TENSOR II spectrometry was used for FTIR measurements.

### 3. Results and Discussion

Figure 4(a) shows the XRD spectrum that corresponds to the Bi<sub>2</sub>Te<sub>2.4</sub>Se<sub>0.6</sub> specimen. The compare XRD data with machine reference code 98-061-7110 are displayed in Figure 4(b). It was found that the main reflections were quite well indexed to the reference code. The X-ray diffraction (XRD) measure provides the researcher with a fast analytical technique. It defines a phase identification of crystalline material and can give information on crystalline size and lattice train. Figure 4 shows the XRD spectra of Bi<sub>2</sub>Te<sub>2.4</sub>Se<sub>0.6</sub> nanocrystalline materials.

It was found that the main reflections were quite well indexed to the reference code. There were no other crystalline impurities detected which indicated the phase purity of the Bi<sub>2</sub>Te<sub>2.4</sub>Se<sub>0.6</sub> nanopowders. The spectrum revealed that the structure was nano crystalline with a (015) preferred orientation (peak having higher intensity). In order to compare the spectrum with the Bi<sub>2</sub>Te<sub>2.4</sub>Se<sub>0.6</sub> nanostructure standard reference code, corresponding to (101), (015), (1010), (0111), (110), (0015), (205), (0210), (1115) and (125) planes were similar that were in very good agreement with other researcher reports (Shalev et al. 2015).

The diffraction peak broadening demonstrated that the samples are nanocrystalline. Nanocrystalline crystallites are commonly observed as residing the two structurally distinct (Di Monte and Kaspar 2005), especially a single-crystal grain core and a surface shell layer that are defined by a remarkable atom fluctuations at the strained exterior. Moreover, scattering centers give diffraction fringes that cause “diffraction” in three sizes consequently. These diffraction fringes commence off being wider broad at low interference and become unlimitedly sharp at infinite interference. For this reason, in order to define the crystallite dimension, the use of the peak broader is restricted to cases.

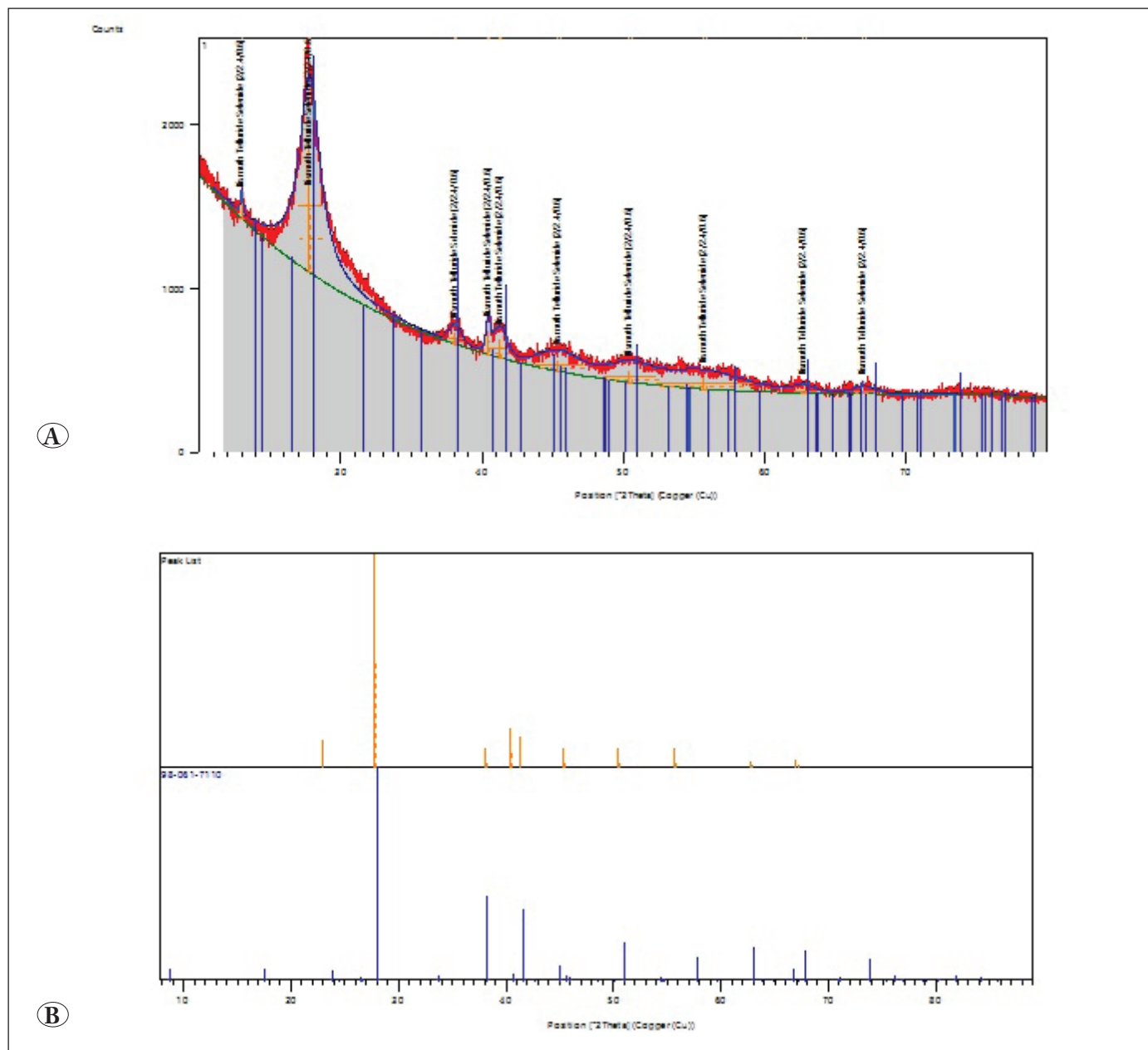


**Figure 4.** XRD spectra of Bi<sub>2</sub>Te<sub>2.5</sub>Se<sub>0.6</sub> nanostructures. **A)** XRD Spectrum. **B)** Compare the result with machine reference code.

The secondly utilized source for specimen broad is tension. If the crystallite is tensioned then the d spacing's will be varied; a compressive tension would make the d spacing's smaller, say reducing a given spacing  $d$  to  $d-\delta d$ . The crystalline dimension and lattice train were estimated with well-known Scherrer equation (Burton et al. 2009) using the (015) reflection is 4.86 nm and 0.0310, respectively, which conforms reasonably well to the nanostructure form (Li et al. 2013, Gharsallah et al. 2017).

There were not any apparent variations seen in XRD patterns for  $\text{Bi}_2\text{Te}_{2.4}\text{Se}_{0.6}$  nanostructure as compared with that of  $\text{Bi}_2\text{Te}_3$ . This experimental results indicated that maximum of the placed specimens had the same crystallographic form as  $\text{Bi}_2\text{Te}_3$ . It was recommended that Se doped  $\text{Bi}_2\text{Te}_3$  was a productive way for decreasing the thermal conductivity when it was compared to  $\text{Bi}_2\text{Te}_3$  presumably owing to the developed phonon scatterings.

The SEM image was applied to determine the morphological and microstructural information about the prepared

sample. Figure 5 shows the SEM image of Bi<sub>2</sub>Te<sub>2.4</sub>Se<sub>0.6</sub> nanostructures, the homogeneity of the sample was arranged sequentially which shows that nanostructures are well agglomerated.

The sample was formed of polyhedral agglomerate. Also the samples have single crystalline apparently. The low thermal conductivity of this material was produced by providing many surface boundaries, which increased phonon scattering. It could be seen that the grains of Bi<sub>2</sub>Te<sub>2.4</sub>Se<sub>0.6</sub> exhibited initial powder morphologies, quasi spherical granule shapes in agglomerated clusters and the grain dimensions were still in nanometer range according to the other researcher reports (Guo et al. 2016, Li et al. 2012, Lognone and Gascoin 2015). It showed a stacking of nanosized particles and crystalline form with broad smooth surfaces to the crystallographic axis. This nanostructuration notably influenced the TE properties; involve abounding surface boundaries that were responsible for broad phonon scattering circumstance.

The EDX was utilized to identify the atomic elemental composition of Bi<sub>2</sub>Te<sub>2.4</sub>Se<sub>0.6</sub> nanostructure. The EDX analysis was also crucial for improved accuracy of the

quantitative compounds. Figure 6 shows the EDX spectrum that materials of Bi, Te and Se were arranged with their atomic stoichiometric ratio. From these curve, it was also confirmed that Bi<sub>2</sub>Te<sub>2.4</sub>Se<sub>0.6</sub> nanocrystalline identified Bi, Te and Se which was in good agreement with other reports (Adam et al. 2017).

TEM is the most powerful technique for the characterization of nanoparticle size, composition and crystalline structure. When an electron beam interacts with a sample, the electrons can be transmitted, scattered, backscattered or diffracted (Carter and Williams 2009, Frenkel et al. 2001). TEM uses the transmitted electron signal to form an image of the specimen. The transmitted electron beam is dependent on the sample thickness; for thin samples (a few nanometers), the transmitted electrons pass through without significant energy loss. Figure 7 shows the TEM spectra of Bi<sub>2</sub>Te<sub>2.4</sub>Se<sub>0.6</sub> nanostructures that exhibited an aggregate phenomenon, and the primary crystalline size is about low dimension.

The most important properties of a semiconductor nanostructure material are its optical behavior to crystalline dimension. While interacting with infrared light causes molecules to undergo vibrational transition, the shorter

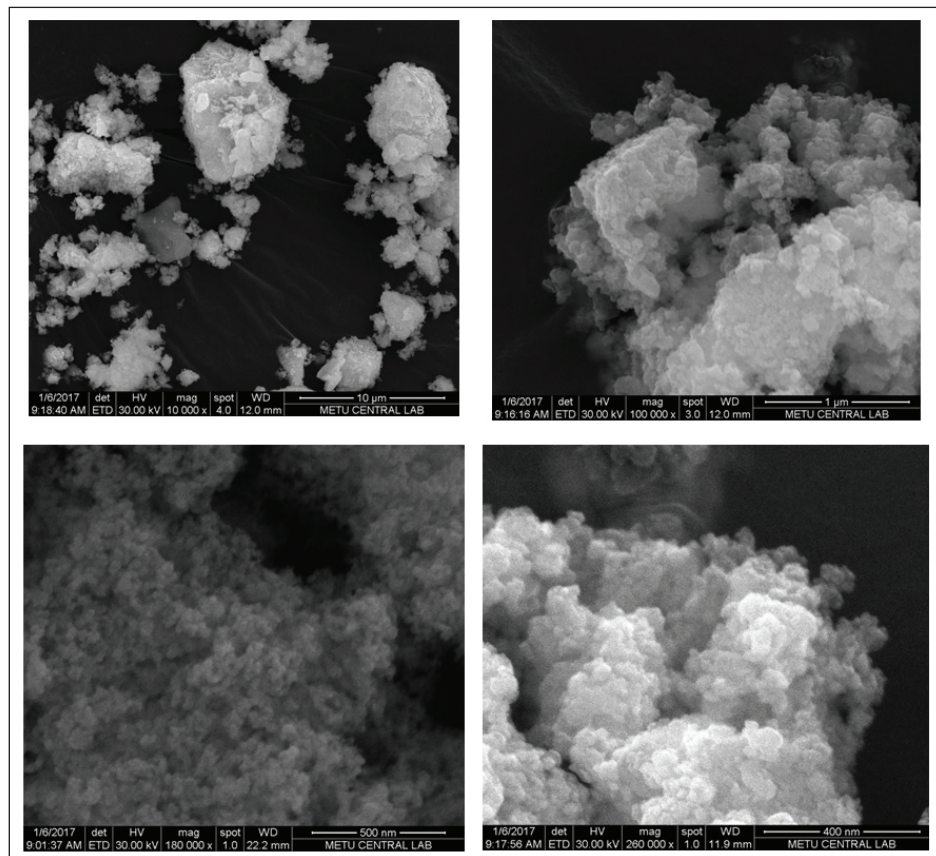


**Figure 5.** SEM spectra of Bi<sub>2</sub>Te<sub>2.4</sub>Se<sub>0.6</sub> nanostructures.

wavelength of the electromagnetic spectrum causes many organic molecules to undergo electronic transition. The UV-visible absorbance spectrum was recorded between 200 and 800 nm for the prepared sample. The absorbance spectrum is shown in Figure 9 for Bi<sub>2</sub>Te<sub>2.4</sub>Se<sub>0.6</sub> nanostructures. The

prominent absorption was found between 200 and 235 nm which may be due to the quantum confinement consequence in the nanostructure materials. The light moves to the blue end of the spectrum, as its wavelengths get shorter that represents the ‘blue shift’ formation. The blue shift may be

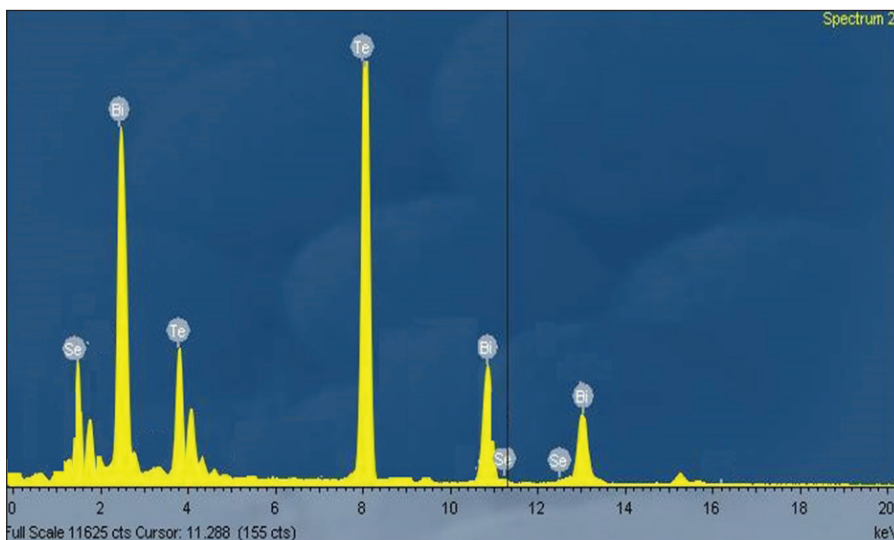


**Figure 6.** EDX spectrum of Bi<sub>2</sub>Te<sub>2.4</sub>Se<sub>0.6</sub> nanostructures.

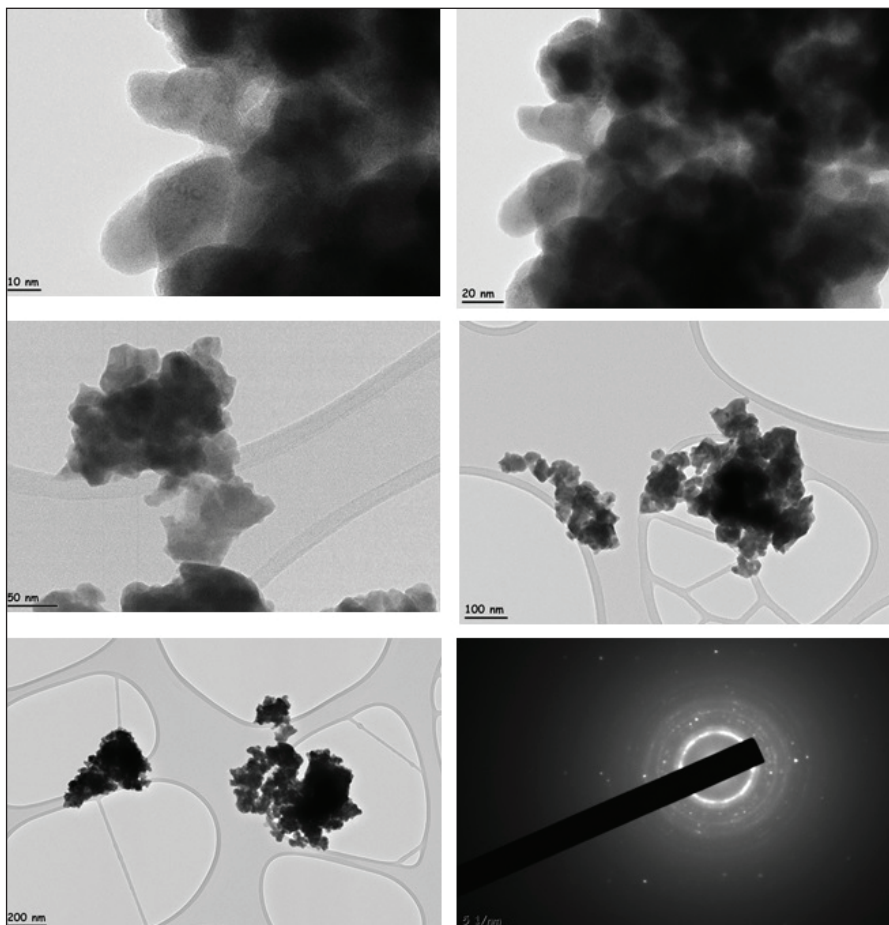


**Figure 7.** TEM spectra of Bi<sub>2</sub>Te<sub>2.4</sub>Se<sub>0.6</sub> nanostructures.

caused by nano dimensional effect (Chen et al. 2012, Hyeon et al. 2001). As the crystalline dimension is decreased, the electronic states are discretized and result in widening of the energy gap and increase the oscillator strength. These

features known as quantum size effect are observed in semiconductor nanocrystals. Hence, quantum size effect is increased by the band gap energy.

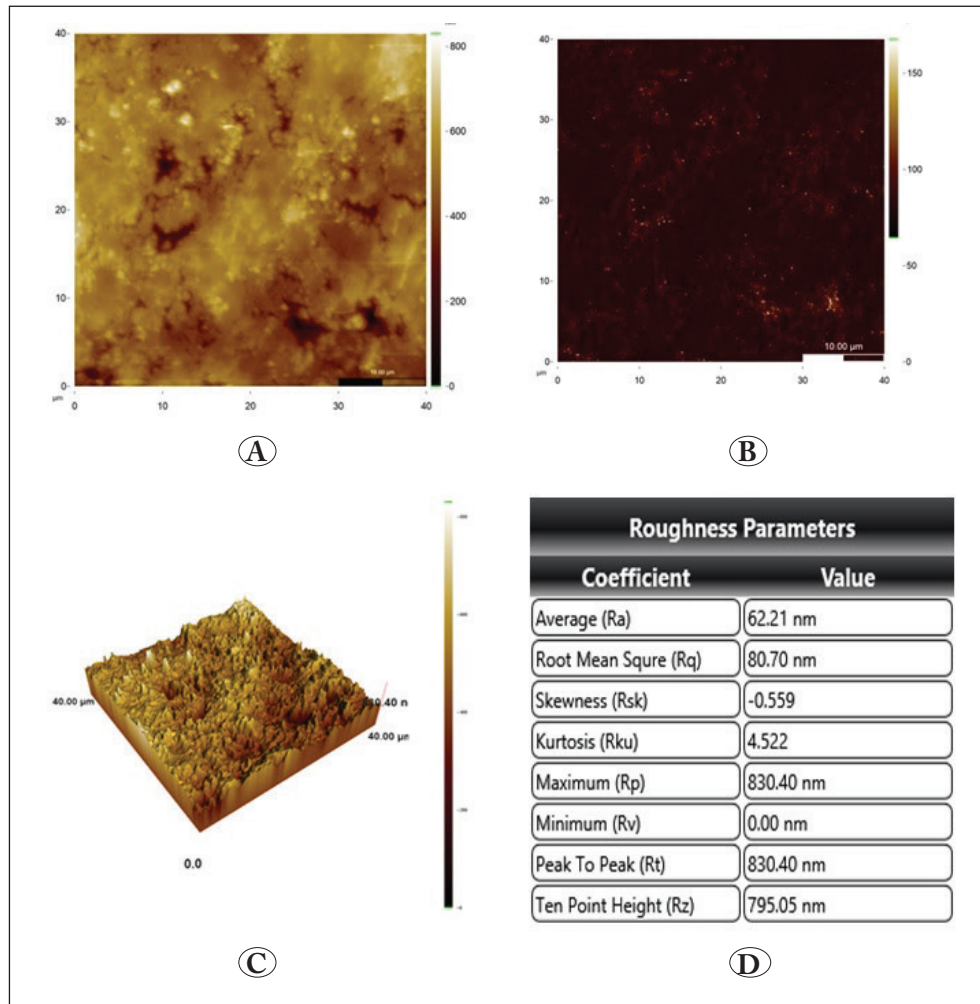


**Figure 8.** AFM spectrum of Bi<sub>2</sub>Te<sub>2.4</sub>Se<sub>0.6</sub> nanostructure pellet.

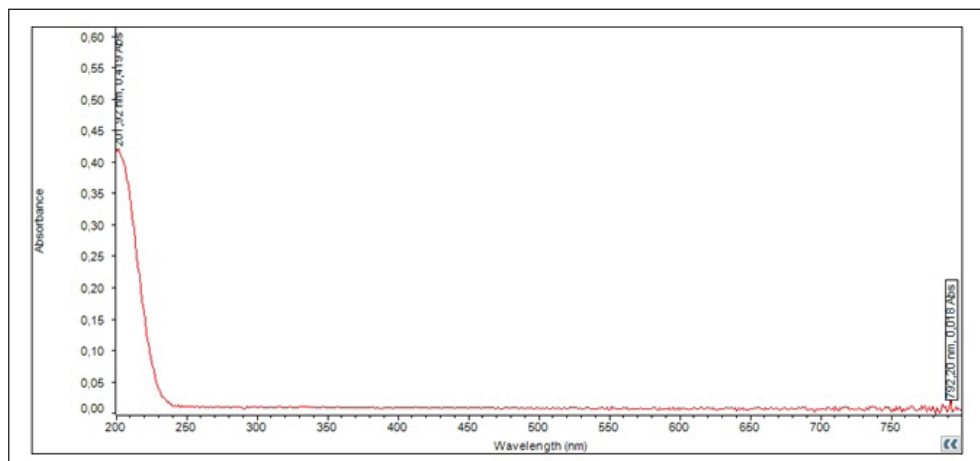


**Figure 9.** UV spectrum of Bi<sub>2</sub>Te<sub>2.4</sub>Se<sub>0.6</sub> nanostructures.

Figure 10 shows the FTIR transmittance spectra of Bi<sub>2</sub>Te<sub>2.4</sub>Se<sub>0.6</sub> nanostructures. The chemical bonds had characteristic frequencies at which they vibrate. They can be set on vibrations by illuminating the sample with infra-red light at the right frequency.

From Figure 10, it can be seen that these corresponding peaks from 400 cm<sup>-1</sup> to 200 cm<sup>-1</sup> on the sample were assigned to C-S, C-O, O-H and C=O stretching, respectively. The peaks at 2326.01 cm<sup>-1</sup>, 2115.34 cm<sup>-1</sup> and 1992.54 cm<sup>-1</sup> were assigned to triple bond regime that C-C and C-N. Identify other major peaks at 1165.85 cm<sup>-1</sup>, 749.47 cm<sup>-1</sup> and 493.43 cm<sup>-1</sup> were assigned to the finger print. Compare the FTIR spectrum with the reference Bi<sub>2</sub>Te<sub>3</sub> and Bi<sub>2</sub>Se<sub>3</sub> nanostructure that the C-C, and C-N stretching was well match (Molli et al. 2012).

The nanoparticles are the range from 0.5 nm to above in diameter has been characterized by AFM studies. An outstanding feature of the AFM is that it can directly create images of nanoparticles. Nanoparticle roughness parameters are directly calculated from AFM images. These parameters were observed by AFM studies that shown in Figure 8. The surface roughness plays an important influence in determining optical scattering and absorption, electrical resistivity and crystalline dimension. The interfacial properties are also influenced by the surface structure. The AFM spectra show that the sample is nanocrystalline and uniform grains. There is no anomalous broad crystallization and the appearance of crystalline dimension is narrow. Material with a narrow crystalline dimension was appreciated to maximize the

potential for grain boundary. The nanocrystalline materials indicate the high strength and low ductility properties of the sample. It is suggested that a more conductive exterior could help to advance the precursor decompositions. This facilitates the formation of exterior complexes and the average roughness value is about 62.21 nm.

#### 4. Conclusions and Future Perspective

In summary, a simple two-step co-precipitation chemical route was developed and successfully established to synthesize Bi<sub>2</sub>Te<sub>2.4</sub>Se<sub>0.6</sub> nanostructures. The precursor was reduced by NaBH<sub>4</sub> to produce ultra-fine particle. Furthermore, the experimental results revealed that the sample exhibited the nanocrystalline form that crystalline dimension of about 5 nm. This method is easy, adequate, less precarious and inexpensive correlate to the other route.

Seebeck coefficient also changes as TEGs become nanoscale. Their figure of merit value is increasing. Thus, they are becoming more widespread to contribute to energy efficiency in waste heat recovery. The electrical and thermal tests of the nano-scale models will be carried out at a later stage. Furthermore, according to the positive results obtained from these, the production of the TEG is the target of the work carried out.

#### 5. Acknowledgments

This work was supported by the Manisa Celal Bayar University, Scientific Research Projects. Coordination Unit, No: 2016-147. We are grateful to the University Authority.

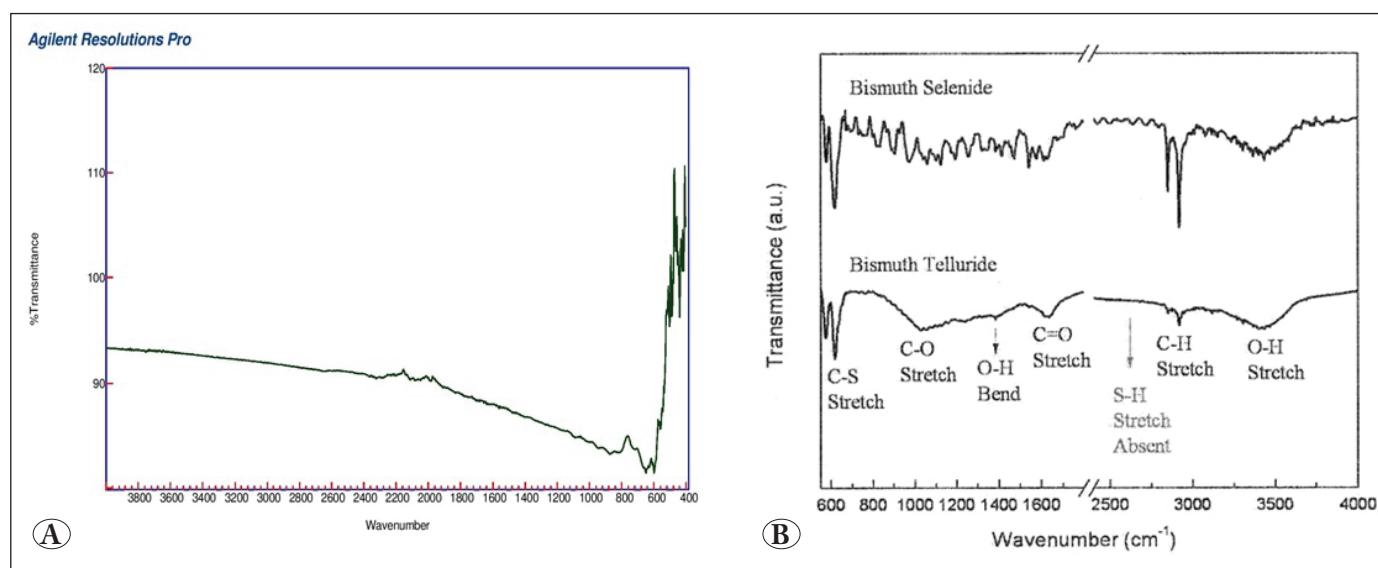


**Figure 10.** FT-IR spectra of Bi<sub>2</sub>Te<sub>2.4</sub>Se<sub>0.6</sub> nanostructures. **A)** FTIR spectrum. **B)** Compare the result with a standard reference.

## 7. References

- Adam, AM., Lilov, E., Petkov, P.** 2017. Optical and thermoelectric properties of nano-particles based Bi<sub>2</sub>(Te<sub>1-x</sub>Se<sub>x</sub>)<sub>3</sub> thin films. *Superlattice Microst.*, 101:609–624.
- Barman, SC., Saha, DK., Mamur, H., Bhuiyan, MRA.** 2016. Growth and description of Cu nanostructure via a chemical reducing process. *J. Nanosci. Nano Engg. Appl.*, 6:27–31.
- Bhuiyan, MRA., Alam, MM., Momin, MA., Uddin, MJ., Islam, M.** 2012. Synthesis and characterization of barrium titanate (BaTiO<sub>3</sub>) nanoparticle. *Int. J. Mater. Mech. Engg.*, 1:21–24.
- Bhuiyan, MRA., Alam, MM., Momin, MA., Rahman, MK., Saha, DK.** 2014. Growth and characterization of CuInSe<sub>2</sub> nanoparticles for solar cell applications. *J. Alter. Energ. Sour. Tech.*, 5:13–17.
- Bhuiyan, MRA., Rahman, MK.** 2014. Synthesis and characterization of Ni doped ZnO nanoparticles. *Int. J. Engg. Manuf.*, 3:67–73.
- Bhuiyan, MRA., Mamur, H.,** 2016. Review of the bismuth telluride (Bi<sub>2</sub>Te<sub>3</sub>) nanoparticle: Growth and characterization. *Int. J. Energy Appl. Tech.*, 3:27–31.
- Bhuiyan, MRA., Alam, MM., Momin, MA., Mamur, H.** 2017. Characterization of Al doped ZnO nanostructures via an electrochemical route. *Int. J. Energy Appl. Tech.*, 4:28–33.
- Bisquert, J.** 2008. Physical electrochemistry of nanostructured devices. *Phys. Chem. Chem. Phys.*, 10:49–72.
- Burton, AW., Ong, K., Rea, T., Chan, IY.** 2009. On the estimation of average crystallite size of zeolites from the Scherrer equation: a critical evaluation of its application to zeolites with one-dimensional pore systems. *Micropor. Mesopor. Mat.*, 117:75–90.
- Carter, CB., Williams, DB.** 2009. Transmission Electron Microscopy, 2nd edn, Springer: US.
- Chen, L., Zhao, Q., Ruan, X.** 2012. Facile synthesis of ultra-small Bi<sub>2</sub>Te<sub>3</sub> nanoparticles, nanorods and nanoplates and their morphology-dependent Raman spectroscopy. *Mater. Lett.*, 82:112–115.
- Di Monte, R., Kašpar, J.** 2005. Nanostructured CeO<sub>2</sub>–ZrO<sub>2</sub> mixed oxides. *J. Mater. Chem.*, 15:633–648.
- Frenkel, AI., Hills CW., Nuzzo, RG.** 2001. A View from the Inside: complexity in the atomic scale ordering of supported metal nanoparticles. *J. Phys. Chem. B*, 105:12689–12703.
- Gharsallah, M., Serrano-Sánchez, F., Nemes, NM., Martinez, JL., Alonso, JA.** 2017. Influence of doping and nanostructuration on n-Type Bi<sub>2</sub>(Te<sub>0.8</sub>Se<sub>0.2</sub>)<sub>3</sub> alloys synthesized by arc melting. *Nanoscale Res. Lett.*, 12:47–54.
- Guo, J., Jian, J., Zhang, Z., Wu, R., Li, J., Sun, Y.** 2016. Thin single-crystalline Bi<sub>2</sub>(Te<sub>1-x</sub>Se<sub>x</sub>)<sub>3</sub> ternary nanosheets synthesized by a solvothermal technique. *J. Cryst. Growth*, 434:1–6.
- Huang, XJ., Choi, YK.** 2007. Chemical sensors based on nanostructured materials, *Sensor. Actuat. B-Chem.*, 122:659–671.
- Hyeon, T., Lee, SS., Park, J., Chung, Y., Na, HB.** 2001. Synthesis of highly crystalline and monodisperse maghemite nanocrystallites without a size-selection process. *J. Am. Chem. Soc.*, 123:12798–12801.
- Ivanova, LD., Granatkina, YV., Petrova, LI., Nikhezina, IY., Malchev, AG., Alenkov, VV., Kichik, SA., Melnikov, AA.** 2017. Thermoelectric properties of Bi<sub>2</sub>Te<sub>2.4</sub>Se<sub>0.6</sub> solid solutions of different particle-size composition. *Semiconductors+*, 51:1002–1008.
- Ju, H., Kim, J.** 2016. Preparation and structure dependent thermoelectric properties of nanostructured bulk bismuth telluride with grapheme. *J. Alloys Compd.*, 664:639–647.
- Klimovskikh, II., Sostina, D., Petukhov, A., Rybkin, AG., Eremeev, SV., Chulkov, EV., Tereshchenko, OE., Kokh, KA., Shikin, AM.** 2017. Spin-resolved band structure of heterojunction Bi–bilayer/3D topological insulator in the quantum dimension regime in annealed Bi<sub>2</sub>Te<sub>2.4</sub>Se<sub>0.6</sub>. *Sci. Rep. UK*, 7:45797.
- Kumar, P., Pfeffer, M., Peranio, N., Eibl, O., Bäßler, S., Reith, H., Nielsch, K.** 2017. Ternary, single-crystalline Bi<sub>2</sub>(Te,Se)<sub>3</sub> nanowires grown by electrodeposition. *Acta Mater.*, 125:238–245.
- Li, D., Qin, XY., Dou, YC., Li, XY., Sun, RR., Wang, QQ., Li, LL., Xin, HX., Wang, N., Wang, NN., Song, CJ.** 2012. Thermoelectric properties of hydrothermally synthesized Bi<sub>2</sub>Te<sub>3-x</sub>Se<sub>x</sub> (0.6≤x≤0.75) nanocrystals, *Scripta Mater.*, 67:161–164.
- Li, D., Qin, XY., Liu, YF., Wang, NN., Song, CJ., Sun, RR.** 2013. Improved thermoelectric properties for solution grown Bi<sub>2</sub>Te<sub>3-x</sub>Se<sub>x</sub> (0.6≤x≤0.75) nanoplatelet composites. *RSC Adv.*, 3:2632–2638.
- Lognoné, Q., Gascoin, F.** 2015. On the effect of carbon nanotubes on the thermoelectric properties of n-Bi<sub>2</sub>Te<sub>2.4</sub>Se<sub>0.6</sub> made by mechanical alloying. *J. Alloys Compd.*, 635:107–111.
- Lu, K., Lu, J.** 2004. Nanostructured surface layer on metallic materials induced by surface mechanical attrition treatment. *Mater. Sci. Engg. A*, 375:38–45.
- Mamur, H., Bhuiyan, MRA., Korkmaz, F., Nil, M.** 2018. A review on bismuth telluride (Bi<sub>2</sub>Te<sub>3</sub>) nanostructure for thermoelectric applications, *Renew. Sust. Energ. Rev.*, 82, 4159–4169.

- Meroz, O., Ben-Ayoun, D., Beeri, O., Gelbstein, Y. 2016.** Development of Bi<sub>2</sub>Te<sub>2.4</sub>Se<sub>0.6</sub> alloy for thermoelectric power generation applications. *J. Alloys Compd.*, 679:196–201.
- Molli, M., Parola, S., Chunduri, LA., Aditha, S., Muthukumar, VS., Rattan, TM., Kamisetti, V. 2012.** Solvothermal synthesis and study of nonlinear optical properties of nanocrystalline thallium doped bismuth telluride. *J. Solid State Chem.*, 189:85–89.
- Nomura, M., Nakagawa, J., Kage, Y., Maire, J., Moser, D., Paul, O. 2015.** Thermal phonon transport in silicon nanowires and two-dimensional phononic crystal nanostructures. *Appl. Phys. Lett.*, 106:143102.
- Park, JW., Nguyen, ST., Luan, Y., Noh, JS. 2016.** Crystalline bismuth telluride nanoparticles grown by a magnetically assisted physical method. *Mater. Design*, 110:449–455.
- Shalev, T., Meroz, O., Beeri, O., Gelbstein, Y. 2015.** Investigation of the Effect of MoSe<sub>2</sub> on the thermoelectric properties of n-type Bi<sub>2</sub>Te<sub>2.4</sub>Se<sub>0.6</sub>. *J. Electron. Mater.*, 44:1402–1407.
- Şışman, İ., Başoğlu, A. 2016.** Effect of Se content on the structural, morphological and optical properties of Bi<sub>2</sub>Te<sub>3-y</sub>Se<sub>y</sub> thin films electrodeposited by under potential deposition technique. *Mater. Sci. Semi. Proc.*, 54:57–64.
- Zhang, G., Kirk, B., Jauregui, LA., Yang, H., Xu, X., Chen, YP., Wu, Y. 2011.** Rational synthesis of ultrathin n-type Bi<sub>2</sub>Te<sub>3</sub> nanowires with enhanced thermoelectric properties. *Nano Lett.*, 12:56–60.